Microgels: Model Polymers for the Cross-Linked State

Markus Antonietti* and Wolfgang Bremser

Institut für Physikalische Chemie der Universität Mainz, Jakob Welder Weg 15, D-6500 Mainz, West Germany

Manfred Schmidt

Max-Planck-Institut für Polymerforschung, Ackermannweg 11, D-6500 Mainz, West Germany

Received August 11, 1989; Revised Manuscript Received February 12, 1990

ABSTRACT: Polystyrene microgels, small network particles with an overall size in the region of 100 nm, are synthesized via radical copolymerization of styrene and *m*-diisopropenylbenzene in microemulsion. The resulting structures are characterized by viscosimetry, static and dynamic light scattering (LS), and dynamic mechanical experiments. These microgels represent strictly spherical particles with a moderate polydispersity where the size of the microemulsion droplets can only be adjusted in the restricted range 60 nm < d < 200 nm. This is possibly due to the polymeric surfactant used. The intrinsic viscosity data are related to molecular swelling where the internal density of the particles in dependence of the cross-linking density obeys the rules of rubber elasticity. From LS experiments it is concluded that the swelling occurs heterogeneously even on the size scale given by the microgel dimensions. The application of microgels as a model for macroscopic networks is extended to the examination of the influence of dilution during the cross-linking reaction. The efficiency of cross-linking decreases with increasing amount of solvent. Dynamic mechanical shear experiments of microgels result in a typical rubbery plateau at high frequencies and small strains known also from macroscopic networks. The absolute plateau value indicates a large amount of defects reducing the cycle rank of the network. Dilution during cross-linking causes a qualitative change of the complete spectrum, which exhibits a continuous loss of the moduli toward lower frequencies, a behavior known for systems close to gel transition.

(I) Introduction

Polymer networks rank among the oldest known synthetic materials: vulcanized rubber or bakelite are just two very different exponents of this class. Contrary to linear polymers with a comparable chemistry, new properties arise from the fact that these substances are covalently cross-linked. The combination of the resulting fixed geometry or topological arrangement of the elementary chains with a local, fluidlike mobility of the polymer segments leads to many interesting applications. For instance, mechanical deformation is reversible, and a large part of the stored energy becomes recoverable.

However, in contrast to the simple chemical reactions involved, cross-linking frequently produces structures with extremely complicated topologies. For illustration, Figure 1 sketches three very simple two-dimensionally cross-linked structures which differ in the geometrical arrangement of the network-forming elements. The chemical composition of these networks could be identical because the cross-linking reactions can be preformed with the same reactants. However, due to their different topologies, these structures will exhibit completely different structural and dynamic properties. It should be noted that the topologies shown in Figure 1 are selected from a vast variety of possible structures, differing either in the chemical cross-linking topology or in the interpenetration of the network meshes without direct covalent cross-linking.

Although many important properties of a polymer network do originate from the topological structure, almost nothing is known quantitatively about the topological contribution to network behavior. This deficiency is caused by the macroscopic nature of networks, which renders quantitative statements very difficult. Small-angle neutron scattering experiments on model networks[1] have indicated that the structure is far more complicated than is usually

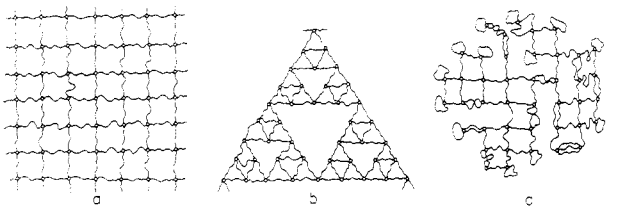

Figure 1. Simple examples for diverse network topologies in two dimensions: (a) the "fishing net"; (b) the Sierpinski gasket; (c) a network with "small" defects. For simplicity, the network functionality (f = 4) and the elementary chain length were chosen to be the same in all cases.

modeled by grid-type arrangements that are inherently applied to the theoretical descriptions of network behavior. In this context even a "fractal" nature of polymer networks is discussed.

On the other hand, the concept of "trapped" entanglements is frequently used to explain deviations from theoretically expected behavior.[2] Of course this description remains a first approximation to the real topological state.

In the present work we apply a different approach to deepen the understanding of this special group of problems. We have avoided the difficulties arising from the macroscopic nature of networks by preparing microscopic model systems, the so-called microgels. Microgels are small network particles with diameters smaller than 1 μm (typically in the 100-nm region) for which the inner structure resembles typical networks. Due to their molecular nature, they dissolve (networks only become swollen), and they are much easier to handle and purify than their macroscopic counterparts. Generally, systems with an overall size in this region are also called "mesoscopic"[3] since many of their physical properties are intermediate between macroscopic structures and "microscopic" molecular fluids. However, we keep the notation microscopic or microgels to remain consistent with

0024-9297/90/2223-3796$02.50/0

previous works and since their synthesis occurs in a microemulsion.

The synthesis of microgels was described by Staudinger as early as 1935;[4] however, it took until 1974 before Hoffmann[5] made the first systematic examinations of microgels for the characterization of branched polymers. In this paper we will restrict ourselves to the characterization of highly cross-linked structures, since the solubility allows typical network properties to be analyzed by the classical methods of polymer characterization.

Among others, static and dynamic light scattering provides a detailed characterization of linear, branched, and cross-linked macromolecules in solution. Although the measurable quantities can be more accurately determined as the particle size increases, an upper limit is imposed by the occurrence of Mie scattering, which complicates the data analysis considerably.

On the other hand, the particle size must be sufficiently large to ensure that all structure elements of the corresponding macroscopic network do occur in the microgels as well. Moreover, surface effects may influence the microgel properties. Consequently, different microgel sizes should be investigated, and, if necessary, the measured properties should be extrapolated to infinite molecular mass. During the experiments it became apparent that particles with diameters of 50–250 nm fulfill most of these demanded conditions.

For those reasons we will present a method for the controlled synthesis of microgels with a defined size. The reaction conditions are similar to those applied to the usual macroscopic network synthesis. As additional experimental parameters we vary the method and density of cross-linking. The resulting microgels will be characterized with simultaneous static and dynamic light scattering, solution viscosimetry, and rheological experiments in the bulk. From the combination of these experiments we expect a deeper insight into the relationship between cross-linking topology and the applied reaction conditions for all cross-linked systems.

(II) Experimental Section

(II.1) Polymer Synthesis. Microgels with a well-defined structure are simply prepared by emulsion and microemulsion polymerization where the cross-linking reaction occurs within the restricted volume of a micelle. Size and shape of the resulting microgels are an exact copy of the molecular reaction vessel. We decided to carry out the reaction as a microemulsion polymerization since this technique avoids heterogeneities ("core-shell problem") which can occur during classical emulsion polymerization. The present systems usually consist of styrene/*m*-diisopropenylbenzene (*m*-DIB), a monomer/cross-linker pair with favorable copolymerization parameters.[6] The experimental procedure can be regarded as a standard technique[7-10] and should just briefly be described.

Microemulsions, as classically defined by Schulman,[11] are transparent and thermodynamically stable dispersions of oil, water, and surfactant. For the synthetic aim of this work, this definition is for our feeling slightly misleading. On the one hand, a wide variety of apparently similar phenomena are included within this definition, and it is meaningful to perform further diversification (see, for instance, ref 12). On the other hand, dispersions obeying the same physical rules but forming slightly larger droplets (and consequently with a turbid appearance) are excluded from this definition.

During this work we extend the notation microemulsion to all dispersions of two separated, well-defined phases where the droplet size is a thermodynamically controlled equilibrium property. In addition, the resulting droplets should be sufficiently small to prevent sedimentation within the time range of all experiments. Practically, this restriction results in an upper limit of the droplet diameter of $d \approx 400$ nm, depending on the density difference between the diverse phases. More experimental details related to this subject and a generalized picture of a polymerization in microemulsion will be presented in a forthcoming publication.[13]

Most mixtures that produce microemulsions contain a large amount of ethanol or other alcohols as "cosurfactants" (see, for instance, refs 7 and 8). However, the alcohol also enters the oil phase, resulting in a severe change of network topology as will be shown below. Consequently, such mixtures are inappropriate for the intended examinations. In a recent publication,[10] Thomas et al. describe a one-component surfactant system (cetyltrimethylammonium bromide) that forms microemulsions. Data produced by our group[13] indicate that such systems produce stable microemulsions with particle diameters up to 30 nm but then become unstable at even larger droplet sizes. Therefore, we chose a system that allows the formation of microemulsions with larger droplets at comparably low amounts of surfactant.[14] Here, a polymeric surfactant (Lutensol AT50, a poly(ethylene oxide) derivative) mixed with sodium dodecylsulfate was applied.

For such a polymerization, we typically use 50 g of destabilized styrene, the stoichiometric amount of cross-linker *m*-diisopropenylbenzene, and 0.125 g of a lypophilic starter as AIBN (azobis(isobutyronitrile)). The cross-linking density is twice the molar ratio of cross-linking agent to monomer since any cross-linker is incorporated in two chains. For example, 0.38 g of *m*-DIB per 50 g of styrene is necessary for a cross-linking density of $p_c = 1/100$ or 1 cross-link per 100 monomer units. All components are mixed, thus forming the lipophilic phase. A solution of 7 g of Lutensol AT50 (BASF Co.) and of 2.5 g of SDS (sodium dodecyl sulfate) as a cosurfactant in 200 g of deionized and degassed water is prepared separately. Oil and water phases are dispersed with a high-speed stirrer and are heated afterward to 70 °C. The reaction is completed after 24 h; conversions are typically greater than $p = 0.97$–0.99 as determined by the mass of isolated polymer.

Optical micrographs of such dispersions performed with a dark-field condenser prior to and after polymerization clearly indicate the absence of monomer droplets with sizes above 1 μm. In addition, the change in turbidity during polymerization can be described by the increase of the index of refraction only; consequently, a growth of the microdroplets can be excluded.[13] This is in good agreement with the observations described in ref 8. Although the mixture is very turbid and nontransparent, these facts justify the use of the notation microemulsion as defined above.

In some cases, the oil phase has been diluted by addition of an inert solvent. For instance, 35 g of toluene are added to 15 g of the monomer/cross-linker/initiator mixture, thus forming the new oil phase. After the oil phase was mixed with the water/surfactant phase as described above, we heated the mixture for 3 days to 70 °C for completion.

It should be mentioned that, in contrast to emulsion polymerization, the reaction can be generally started with a lipophilic initiator. The reaction proceeds in the small oil droplets that are already formed from mixing of the emulsion. From a chemical point of view, this is a simple criterion to differentiate between an emulsion and a microemulsion polymerization.

An aliquot of all resulting products is kept for characterization of the latex with electron microscopy and dynamic light scattering, and the remaining portion is precipitated by addition of 200 mL of hot methanol. The surfactants are carefully removed from the product by a 3-fold reprecipitation from THF by using methanol. The resulting white powder is dried in the vacuum oven for 48 h at 60 °C.

Electron micrographs of the latex after polymerization indicate a strictly spherical shape of the particles with a moderate polydispersity of $1.003 < d_w/d_n < 1.05$, depending on the absolute size and the quality of mixing before the start of the reaction. The latter point has to be interpreted as a slow approach to an equilibrium state due to the polymeric surfactant rather than a thermodynamical instability of the microemulsion. These results will be presented in a forthcoming paper.[13]

(II.2) Solution Viscosity Measurements. The viscosity measurements were performed in toluene at 20.0 °C with an automatic Schott AVS300 instrument, which allows the determination of the flow time with an accuracy of 0.01 s. The

Table I
Characterization of the Latex after Polymerization[a]

sample	A50c	A50d	A50a	A50EDM	A20	A50/0.3	A50e
S	0.01	0.02	0.14	0.14	0.14	0.14	0.56
r_H(latex), nm	91.9	71.6	58.7	57.2	51.9	57.2	39.1
b, nm	0.3	0.5	2.5	2.5	2.2	2.5	5.4

[a] r_H is the hydrodynamic radius of the latex after polymerization as determined by dynamic light scattering; b is the apparent layer thickness as calculated from eq 1.

Ubbelohde viscosimeter used in this setup was coated with trichlorooctadecylsilane to avoid particle absorption, which can severely disturb measurements due to the very high molecular weights of the examined systems. The solutions were prepared by dissolving the samples in freshly distilled, sodium-dried toluene. The samples are clarified by a 5-fold filtering procedure through 0.45-μm filters (Sartorius Co.). The flow times were determined for 6–9 concentrations ranging from 5 to 2 g/L.

(II.3) Static and Dynamic Light Scattering. The spectrometer and procedure for simultaneous static and dynamic light scattering are extensively described in previous publications.[15,16] The measurements were performed at the 647.1-nm line of a krypton ion laser (Spectra-Physics 2025). We adopted the refractive index increment from linear polystyrene in toluene, $\partial n/\partial c = 0.110$ ($T = 20$ °C).

Ultimately it turned out that the sample clarification as described in section II.2 for the viscosity measurements was not adequate for the light-scattering investigation, because measurements were performed at much smaller concentration, typically at $10^{-3} \leq c \leq 10^{-2}$ g/L. Coating the cells with trichlorooctadecylsilane did not completely prohibit absorption of the microgels at the walls, which introduced a considerable (time-dependent) concentration error (20–50%). This effect could be neglected for the viscosimetric measurements since the absolute mass of the absorbed polymer is comparably low for the concentrations applied in viscosimetry.

Satisfactory results were obtained by coating the optical quartz cuvettes by the microgel itself, i.e., rinsing the cells with a concentrated solution of the examined microgel, followed by the usual clarification procedure of the cell. Measurements with the pure solvent in the coated cells have shown that the absorbed microgels are not removable under the usual measuring conditions; no microgel particles could be detected that could possibly arise from a time-dependent absorption equilibrium.

The final concentrations range between 10^{-2} and 10^{-3} g/L and are realized by filtering a more concentrated solution through Millipore 0.45-μm Teflon filters into the cuvette and subsequent dilution within the optical cell with a controlled amount of filtered solvent. With this procedure the most accurate and reproducible concentrations are obtained.[17] The molecular mass of the samples is determined by extrapolating data from four different concentrations also covering a factor of 4.

(II.4) Dynamic Mechanical Experiments. The purified microgel powder is molded under compression at 150 °C in a modified IR press until optically clear disks with 13-mm-diameter thickness fitting the geometry of a plate/plate rheometer are obtained. A Rheometrics RMS 800 apparatus was used in an oscillating low-amplitude mode in a frequency range between 10^{-2} and 10^{2} rad·s^{-1} with the amplitude of 2%. For different samples it was checked that the measurements are within the linear regime of mechanical response, which extends minimally up to 10%.

The measurements were controlled by a FRT2000 frequency response analyzer, which also records the complex torque. A stream of dry nitrogen was blown over the sample in order to avoid thermal oxidative damage during the measurements performed at 130–210 °C. After the sample has been heated to the maximum temperature, the measurements at 150 °C have been repeated in order to check for alteration. Compared to linear polystyrene this type of microgel is relatively stable; the data are reproduced within the accuracy of the measurements. The different curves are superimposed on a master curve by using the temperature–frequency superposition principle. Except for temperature and density corrections, only horizontal shifts are applied.

(III) Results and Discussion

(A) Latex Characterization. The dependence of the absolute microgel size on the amount of surfactant has been checked. In Table I, the hydrodynamic radius, $r_H \equiv \langle r_h^{-1} \rangle_z^{-1}$, of the latex of different samples is compared with the weight ratio of surfactant to monomer S. An average surfactant layer thickness, b, is calculated from S with the crude assumption of a uniform distribution for polymeric soap on the surface of the spherical particles using eq 1 where ρ_{surf} and ρ_{polym} are the densities ofsurfactant and

$$S = \frac{m_{surf}}{m_{polym}} = \frac{\rho_{surf}}{\rho_{polym}} \frac{^4/_3\pi R^3 - ^4/_3\pi (R-b)^3}{^4/_3\pi (R-b)^3} \approx \frac{R^3}{(R-b)^3} - 1 \Rightarrow b \approx R(1-(1+S)^{-1/3}) \quad (1)$$

polymer, respectively. This equation is derived from the assumption that the volume of the surfactant phase can be calculated from the formula for hollow spheres. Therefore, this picture provides only a first imprint of the real physical situation since it neglects the existence of free soap molecules or "empty" micelles and also assumes sharp boundaries between oil, surfactant, and water phases. For practical purposes, R can be identified with r_H of the latex. The calculation of b is not affected by polydispersity since the z-average of R is the relevant property for both quantities.

In contrast to the simple expectation and behavior of microemulsions stabilized with low molecular weight surfactants,[13] we observe that the absolute microgel size depends just slightly on the concentration of surfactant. Consequently, the apparent layer thickness increases strongly with the soap content.

A concentration-dependent layer thickness deviating from the behavior of low molecular weight soaps is also known from studies on diverse polymeric surfactants on liquid/liquid interfaces[18] and can be interpreted as the formation of loops with increasing surfactant concentration.

Due to the resulting comparable low apparent layer thicknesses of less than the diameter of the surfactant molecules, systems with a ratio of approximately $S \approx 0.01$ become more polydisperse and finally instable. The reproducibility of the technique is demonstrated in the case of our "standard" mixture at $S = 0.14$. The scattering of the data is possibly due to the very exothermic nature of polymerization, which leads to a noticeable increase of the reaction temperature.

(B) Structure Characterization in Solution. The intrinsic viscosity, $[\eta]$, was determined for all samples in toluene; the results are given in Table II together with the hydrodynamic radius, r_H (from dynamic light scattering), and the radius of gyration, r_G (from static light scattering). The radius of gyration was derived from a Guinier plot of the reduced scattering intensity as $r_G \equiv \langle s^2 \rangle_z^{0.5}$. In most cases the Guinier plot yielded linear curves, which indicates a spherical shape of the particles in the swollen state. A typical example is shown in Figure 2.

Table II
Data for Different Microgels in Toluene at 20.0 °C[a]

sample	A10	A20	A50a	A50b	A100	A200	A400a
p_c	1/10	1/20	1/50	1/50	1/100	1/200	1/400
$[\eta]$, $cm^3 \cdot g^{-1}$	4.2	9.3	15.1	14.8	23.4	35.6	54.0
Q	1.8	3.9	6.3	6.22	9.8	14.9	22.7
M			193×10^6	347×10^6			
M'		185×10^6	196×10^6	337×10^6	264×10^6	541×10^6	170×10^6
r_η, nm			77.2	93.4			
r_G, nm		51.6	57.9	69.2	64.0	99.3	68.7
r_H, nm		64.9	77.7	92.5	99.4	145.1	113.3
P		0.792	0.741	0.738	0.638	0.684	0.606
r_η/r_H			0.993	1.01			

sample	A400b	A1000	A2500	A50DME	A50/0.3
p_c	1/400	1/1000	1/2500	1/50	1/50
$[\eta]$, $cm^3 \cdot g^{-1}$	61.6	112.0	209	28.5	27.2
Q	25.9	47.0	87.8	12.0	11.4
M	194×10^6				
M'	187×10^6	170×10^6	(140×10^6)	190×10^6	154×10^6
r_η, nm	123.5				
r_G, nm	73.6	79.6	125.3	62.5	66.2
r_H, nm	122.3	144.6	167.3	95.0	87.4
P	0.605	0.583	0.749	0.657	0.757
r_η/r_H	1.01				

[a] Notation of symbols: p_c, cross-linking density; $[\eta]$, intrinsic viscosity; Q, swelling ratio; M, molecular mass determined with light scattering; M', molecular mass calculated from $[\eta]$ and r_H; r_η, viscosimetric radius calculated from $[\eta]$; r_H, hydrodynamic radius determined by QELS; r_G, radius of gyration; $P = r_G/r_H$.

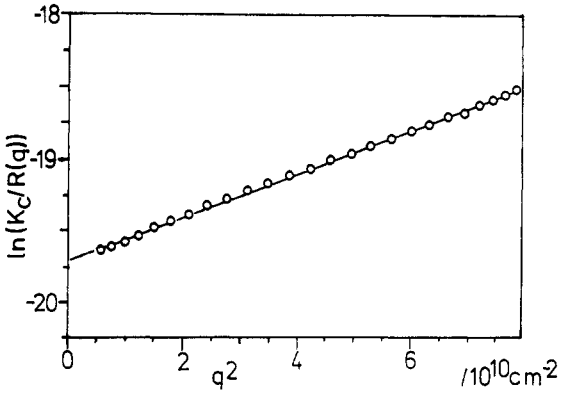

Figure 2. Static light-scattering data on sample A50b presented according to Guinier.

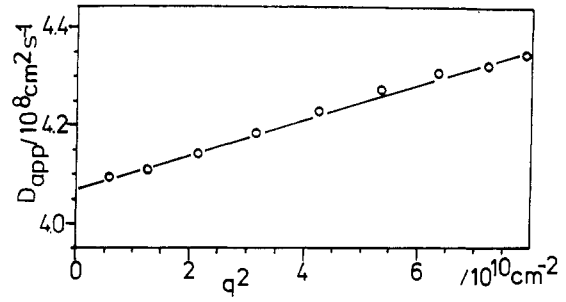

Figure 3. Dynamic light-scattering data of sample A50b as given by the apparent diffusion coefficient versus the square of the scattering vector q.

$r_H \equiv \langle r_H^{-1} \rangle_z^{-1}$ is calculated by the Stokes–Einstein equation from the z-average of the diffusion coefficients determined by dynamic light scattering. The values referred to in Table II are obtained by extrapolating the data to $q \to 0$ and $c \to 0$. Figure 3 sketches a typical example for the extrapolation of such a set of data.

As described above, very small and precise concentrations are experimentally very difficult to achieve due to adsorption losses. Therefore, only three molecular weights have been determined directly by the procedure described in section II.3. Under favorable circumstances

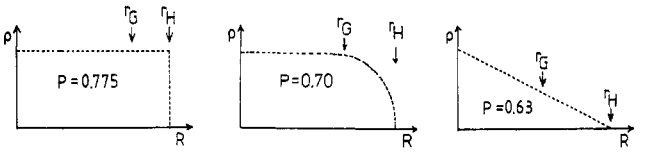

Figure 4. Three simple examples for the radial density function, $\rho(R)$, of spherical structures and the resulting hydrodynamic radii, r_H, and radii of gyration, r_G. The ratio $P = r_G/r_H$ is a sensitive fingerprint of the radial density function.

the molecular weight may be more easily extracted from other quantities such as the hydrodynamic radius and the intrinsic viscosity as will be shown below.

Table II also contains the "viscosimetric" radius, r_η, which is calculated according to eq 2.[19] For spherical microgels, r_η equals r_H. In other words, the Flory–Mandelkern–Scheraga parameter, β[20] (eq 3), is experimentally

$$r_\eta = (3M[\eta]/10\pi N_A)^{1/3} \quad (2)$$

$$\beta = ([\eta]M)^{1/3}/6\pi r_H \quad (3)$$

determined as $\beta = 9.8 \times 10^{-6}$ $mol^{1/3}$, which is exactly the calculated value for a hard sphere. The equivalence of r_H and r_η allows the indirect, but simple, determination of the absolute molecular mass, M', according to eq 1 from $[\eta]$ and r_H. The resulting molecular masses M' are also listed in Table II. The similarity of calculated and measured values in these three cases proves the validity of the applied procedure.

The most predicative information about the inner structure of microgels that are obtained from light scattering is given by the ratio r_G/r_H, the so-called P ratio.[21] Since we have proven that our microgels exhibit radial symmetry, we can discuss the inner architecture by means of the radial density function, $\rho(R)$.

Figure 4 presents three simplified examples for $\rho(R)$, which illustrate the meaning of the P ratio. A homogeneous sphere exhibits a rectangular density function. With the crude assumption that the microgels are hydrodynamically compact (indicated by the equality of r_η and r_H), r_H corresponds to the outer radius of the

sphere, r_A. The radius of gyration, r_G, can be calculated according to the textbook formula of mechanics, and the well-known result $P = 0.775$ is obtained. Similar arguments lead to $P = 0.70$ for a sphere with a "soft" surface, which is modeled by a modified density distribution. Here, the density is given by $\rho(r) = 1 - \exp(-(r - r_A)/\xi)$ for $r \leq r_A$ where the correlation length, ξ, of the surface is taken as $^1/_{10}r_A$. A triangular distribution $\rho(r) = 1 - r/r_A$ for $r \leq r_A$ yields $P = 0.63$. In both cases, the hydrodynamic radius was at will set to $r_H \approx r_A$. This means that hydrodynamic interaction is excluded although the segment density becomes small in the outer regions of the sphere. Any attempt to include hydrodynamic interactions according to Oseen[22] inevitably leads to P values larger than the hard-sphere values in any of the models.

We now compare the experimental P values to these simplified model calculations. For high cross-linking densities the microgels behave essentially like homogeneous spheres. A decrease of the cross-linking densities leads to a decrease of the P ratio. In terms of our crude model calculations, this could mean that the particles become more transient in the outer region; consequently, the particles swell heterogeneously. A P ratio of 0.6 may represent strong evidence that not only is the outer shell of the microgels heterogeneously swollen but also the whole particle is.

Such a proposed heterogeneity should be discussed in relation to the length of the network-forming chains, which is on the order of 5 nm at a cross-linking density of 1/100, and to the number of cross-links in such a particle, which is 25 000 in the case of sample A100/1. Both values are out of the region where heterogeneities can be caused by Gaussian fluctuations of the structure on a scale of the elementary structure units, e.g., dangling chains, a special surface behavior of the outer network meshes or number fluctuations of the cross-linking density.

The nature of these "large-scale" heterogeneities or fluctuations cannot be explored by the data set presented, and further experimental evidence is needed. However, it should be pointed out that most topological arrangements of chains allow a wide distribution of mesh sizes and produce consecutively fluctuations of the local density in the swollen state on a larger scale than the one of the network structure elements as indicated in Figure 1. Only a restricted class of structures, especially all grid-type arrangements, exclude such phenomena, and these architectures can be excluded by our data in turn.

The behavior of the P ratio of sample A2500 is a peculiarity and should not be related to the discussion of the other data. Here, the cross-linking density compared to the primary chain length is so small that a very soft gel is produced; i.e., the sample is very close to its gel point. In this region, however, the structure is expected to lose its spherical shape as experimentally demonstrated by Burchard et al.[23] A more extensive treatment of the structure behavior of microgels close to the gel point will be presented in a forthcoming publication.

(C) "Swelling" Experiments on Microgels and Comparison with Theory. The advantage of investigating microgels rather than macroscopic networks is vividly illustrated by the determination of the swelling ratio, Q. Here, swelling experiments of macroscopic networks are replaced by comparatively simple viscosity determinations.

According to Einstein (eq 4), the intrinsic viscosity, $[\eta]$, measures directly the average mass density within the swollen spherical particles

$$\eta = \eta_s(1 + 2.5\Phi + 4\Phi^2 + 5.5\Phi^3 + ...) \quad (4)$$

$$[\eta] \equiv \lim_{c \to 0} [(\eta - \eta_s)/\eta_s] = 2.5/\rho^* = 2.5Q/\rho \quad (5)$$

where η is the viscosity of the solution, η_s the viscosity of the pure solvent, and Φ the volume fraction of spheres. The swelling ratio, Q, is given by $Q = \rho/\rho^*$, accordingly, with ρ the solid-state density of the polymer and ρ^* the density in the swollen state.

Figure 5 presents the swelling ratios which are dependent upon the average mass of the chains between two cross-links, M_c, calculated from the molar ratio of cross-linker to monomer molecules. Throughout the paper we denote this ratio "chemical" cross-linking density.

According to Flory these data can be linearized as

$$Q^{5/3} - Q/2 = \frac{v_{sp}}{V_s} \frac{M_c}{1 - 2M_c/M_{lin}}(0.5 - \chi) \quad (6)$$

V_s is the molar volume of the solvent, v_{sp} the specific volume of the polymer, and χ the Flory–Huggins interaction parameter between solvent and polymer. M_{lin} is the number-average molecular weight of the primary chain before cross-linking; the complete term corrects for network imperfections due to dangling ends. M_{lin} for our experiments can be determined by performing the microemulsion reaction without cross-linker; the resulting linear chains are characterized with light scattering and GPC to $M_w \approx 950\,000$ and $M_w/M_n \approx 3$. Similar values for the primary chain length were obtained by scission of all cross-links in sample A50/EDM where ethylene glycol dimethacrylate (EDM) was utilized as the cross-linking agent. The scission was performed via transesterification with excess ethanol. The values of M_w determined by GPC and light scattering coincide, which is a good experimental proof for the linear structure of the primary chains.

The agreement between experimental values of the swelling ratio and the theoretical curve in Figure 5 is moderately good. The observed "molecular" swelling ratios also agree quantitatively with values obtained for macroscopic networks with comparable cross-linking densities.[24] In two cases we have checked our procedure for reproducibility: the agreement for the Q values of different microgel charges with the same amount of cross-linker is within 5%.

Figure 5 also considers data of Hoffmann,[5] who first used microgels for the determination of swelling ratios. The parallel shift of the data is most probably due to the solvent quality because salt-containing DMF (Hoffmann) is a poorer solvent for polystyrene than toluene.

It is also possible to calculate the swelling ratio from M_w and r_H, which are measured by static and dynamic light scattering solely. These values agree excellently with our viscosity data, as already seen in $r_\eta/r_H = 1$.

For a more precise comparison of the swelling ratios with theoretical expectations, we can utilize the generalized eq 7. h is the so-called memory term, which corrects for

$$Q = \left[\frac{v_{sp}}{V_s} \frac{0.5 - \chi}{Ah^{2/3} - BQ^{2/3}}\right]^{3/5} \left(\frac{M_c}{1 - 2M_c/M_{lin}}\right)^{3/5} \quad (7)$$

possible swelling effects during cross-linking; for bulk polymerizations h equals 1. A and B are front factors, which depend on the theoretical model.

The historical approach of Flory and Wall[25] results in $A = 1$ and $B = 2/f$, which is identical to eq 6. f is the cross-linking functionality, which is 4 in the present experiments.

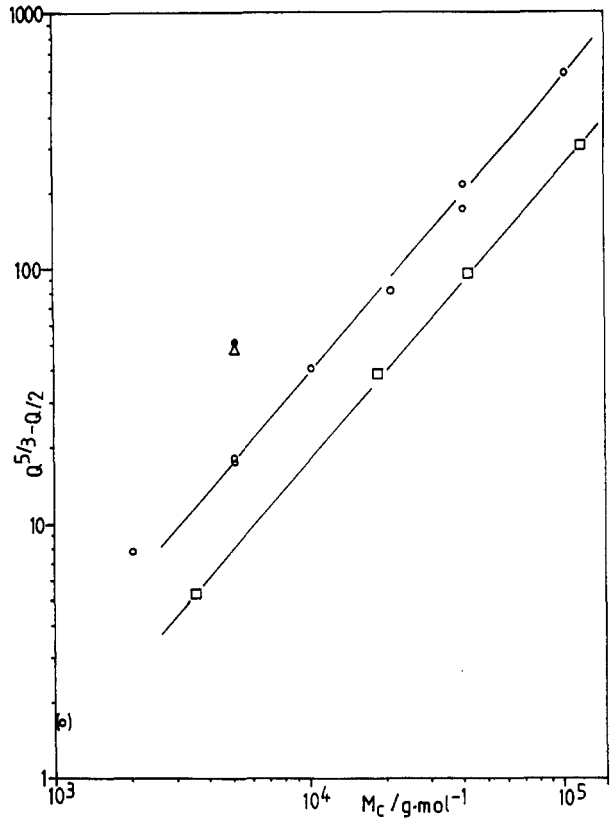

Figure 5. Swelling ratios Q of microgels in dependence of the mass of chain segments M_c between two cross-links linearized by application of the Flory–Wall theory: (○) the values of microgels in toluene at 20 °C as derived from the intrinsic viscosity; (△) sample A50/0.3; (●) A50DME; (□) data taken from the literature[5] for microgels in DMF at 20 °C.

Table III
Apparent χ Values Calculated from the Swelling Ratios by Application of Diverse Theoretical Treatments

sample	Flory–Wall	Hermans	James–Guth	Graessley, Duiser–Staverman	eff_{app}
A20	0.166	0.272	0.323	0.428	0.99
A50a	0.159	0.226	0.322	0.389	0.76
A50b	0.174	0.240	0.331	0.397	0.80
A100	0.122	0.173	0.303	0.353	0.60
A200	0.127	0.162	0.307	0.342	0.57
A400a	0.173	0.196	0.332	0.355	0.66
A400b	0.086	0.111	0.286	0.312	0.57
A1000	0.296	0.305	0.397	0.406	0.92

The theory of Hermans[26] leads to $A = 1$ and $B = 1$, whereas the calculations of James and Guth[27] amount to $A = (f - 2)/f$ and $B = 0$. Finally, the calculations of Graessley[28] and Duiser–Staverman[29] produce $A = (f - 2)/f$ and $B = 2/f$. In all cases end-group corrections similar to eq 6 are applied to obtain a corrected M_c.

Assuming the chemical cross-linking densities as the "real" ones, we can calculate the interaction parameters χ between toluene and the different microgels from these equations, which are shown in Table III. These values ought to be compared to the literature value for χ of the system polystyrene/toluene of $\chi = 0.432$,[30] determined for linear polystyrene chains in dilute solution.

The best agreement between data and theory can be made with the approaches of Graessley and Duiser–Staverman, whereas the simple Flory theory or also the Hermans prediction deviate significantly beyond experimental error. This latter comparison results in a negative χ value at low cross-linking densities where networks should behave most ideally. It is known from examinations of macroscopic PDMS model networks[31,32] that the swelling data, in general, can be better described with "nonaffine" theories (Graessley–Staverman, $A = 0.5$ for $f = 4$); the referred experimental value of $A \approx 0.6$ is close to our results. As in the PDMS experiments, we cannot detect an influence of "trapped" entanglements (which would act as additional cross-links) on the swelling behavior. Even at cross-linking densities as low as 1/1000 where the influence of entanglements should be 6 times larger (calculated with M_e(PS) ≈ 18 000 g/mol) than the one of covalent cross-links, no systematic deviation toward lower swelling ratios is observable.

Contrary to these expectations, Q is underestimated by eq 7 with growing chain length between cross-links. This becomes noticeable by the increasingly lower value of χ at larger M_c; the literature value for linear polystyrene chains is approximately obtained just for high cross-linking densities.

This deviation might originate from imperfections of the theory; it can also be caused by the ineffectiveness of the cross-linking reaction. Assuming a constant $\chi = 0.432$, we adopt the Graessley theory in order to calculate apparent cross-linking efficiencies for various cross-linking densities. The results are also presented in Table III. The efficiency is slightly decreasing as the cross-links become more diluted. However, one should be very cautious to interpret this "inefficiency" as chemically nonformed cross-links. We are sure that more than 85% of the pendant vinyl groups have reacted; the experimental evidence for this fact results from experiments where the primary linear chains are so small that the resulting cross-linked structure is close to its gel point. In this region, the Flory–Stockmayer theory[33] directly allows the calculation of the number of cross-links involved in structural cross-linking. These data and the calculation of the efficiency will be presented in a forthcoming publication.

Also, the amount of reaction as determined by the mass of isolated polymer is greater than 0.97; the difference to the value of 0.85 for the pendant vinyl groups is possibly due to the influence of sterical hindrance, which prevents the remaining part from further polymerization.

The real reason for the loss in cross-linking efficiency as seen by the swelling experiments can be far more complicated and is possibly assigned to the nonuniform segment density distribution as indicated by the light-scattering experiments. That is to say, the same non-grid-type arrangements do result not only in a wide mesh size distribution but also in a formal "inefficiency" of cross-links. This problem will be more extensively discussed below in context with mechanical experiments.

In addition to the question of network topology we can also answer some other questions of network synthesis, thus demonstrating the advantage of microgel experiments. One peculiarity is included in Figure 5, representing the result for the sample A50EDM. This sample exhibits a swelling ratio that is much higher than expected for its chemical cross-linking density. For this sample we have utilized the cross-linking agent ethylene glycol dimethacrylate (EDM) instead of *m*-DIB. One possible explanation is given by the fact that, in contrast to *m*-DIB, EDM is very flexible and can react with itself, forming a nine-atom-membered ring. Although this ring size is sterically unfavored, comparison with the other data indicates that more than 50% of all EDM molecules may be lost for structural cross-linking that way. Also the P ratio coincides with a simple reduction of cross-links considering such a side reaction. The loss of efficiency via such a side reaction agrees well with data obtained from anionic homopolymerization of

Table IV
Apparent Efficiency of Cross-Linking for Samples Cross-Linked in Dilution

sample	A50a	A50b	A50/0.7	A50/0.5	A50/0.3
Φ_P	1	1	0.7	0.5	0.3
$[\eta]$	15.1	14.8	16.2	22.7	27.3
eff_{app}	0.76	0.80	0.73	0.35	0.25

EDM at low conversions[34] where 56% of the second double bonds are detectable after the reaction. The difference is possibly due to the altered reaction conditions and the different reactivity of styrene and EDM.

In another set of experiments we have tested the influence of dilution on cross-linking reactions and their topology. In previous experiments[16,35] we have shown that dilution has a remarkable influence on cross-linking: due to the Ziegler dilution law the probability of formation for cyclic substructures is increased. With the present synthetic strategy we can continuously add solvent to the oil phase of the microemulsion and observe its influence on the microgel structure. Table IV recapitulates these data and their dependence on the volume fraction of the toleune solvent. We observe a strong increase in the swelling ratio with increasing amounts of diluent. According to this ratio, an apparent cross-linking efficiency can be calculated, which is also given in Table IV. We observe that addition of solvent successively lowers this efficiency; in the presence of 70% solvent during polymerization only half of all cross-links is seen in the swelling experiment. Below 10% monomer in the oil phase the gel reaction remains subcritical due to the resulting extremely low efficiency: the created structures are much smaller than the microemulsion particles.

The influence of dilution on the topology seems to be more complicated than simple formation of very small rings: compared to A50EDM, which has the same swelling ratio, the P ratio of sample A50/0.3 remains at the level given by A50/1. The cross-linking density is not simply reduced but must be "hidden" in larger cyclic substructures. This point will be discussed later. In general, these data cast doubts on the ideality of cross-linking reactions in solution since moderate dilution ratios lead already to a severe change in the topology and the cross-linking efficiency, and the resulting structures are not as ideal as generally believed. This fact has been known for many years, and many publications concerning this topic are found in the literature. Stockmayer and Weil found as early as 1945 (quoted in ref 36) that ideal behavior is only obtained at infinite polymer concentration, which is only mathematically accessible by extrapolation. In the bulk they obtained an efficiency of 0.87 for cross-linking due to internal cyclization.

J. E. Mark prepared cross-linked PDMS systems in solution but referred only to the very low efficiency of this process.[37] Guided by mechanical measurements, he related a more "simple" topology to solution-cross-linked systems.

At the system styrene/divinylbenzene kinetic examinations[38] have shown that most of the cross-linking molecules that had polymerized in high dilution are not involved in long chain branching. Hoffmann[5] has observed a higher swelling ratio (compared to the samples cross-linked in the bulk) of styrene/divinylbenzene microgels, which are synthesized in the presence of solvent, and has interpreted it as the formation of small cycles. Schmidt and Burchard[38] have calculated cross-linking efficiencies of the system styrene/divinylbenzene, which was anionically polymerized. Their value of $f = 0.059$ at 5% monomer concentration agrees at least with the observation that the present reaction remains subcritical below 10% monomer concentration.

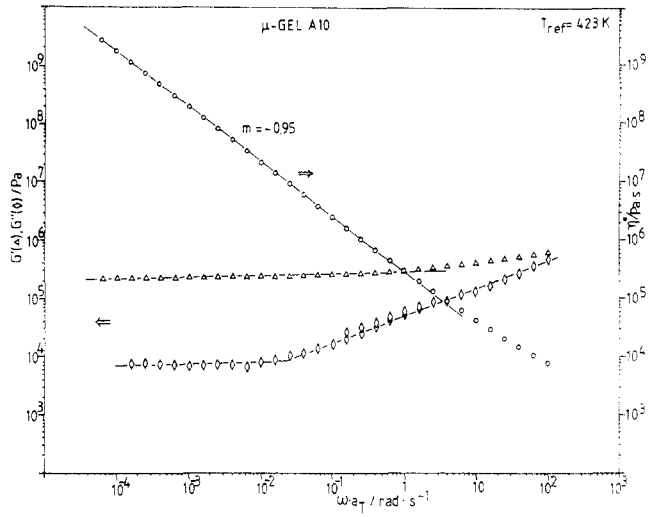

Figure 6. Master curve for sample A10 of the storage modulus, G' (△), the loss modulus, G'' (◇), and the dynamic viscosity, η^* (○), shifted to a reference temperature of T_{ref} = 423 K.

Ilavsky and Dusek[40] have varied the amount of inert diluent during polycondensation of polyurethane networks but found cyclization on the order of 5% in the presence of 60% solvent. Computer simulations of Eichinger and Lee[41] give similar values for the amount of internal small loops. However, it is known that networks made by copolymerization exhibit an enhanced quantity of cyclic substructures compared to end-linked model networks.[42] This observation can be specified by the present experiments: the sensitivity of the cross-linking efficiency on dilution is increased by a factor of 10.

These experiments are far from complete but demonstrate the significance of the general problem and illustrate the fact that a theoretical description for the effects of dilution on cross-linking is still missing. The present memory term $h^{2/3}$ (see eq 6) only corrects for geometrical swelling effects but does not account for internal cyclization. Consequently, our data cannot be expected to be adequately described by these theoretical model calculations.

(D) Characterization with Dynamic Mechanical Experiments. Additional information about the network topology can be obtained also from the dynamic behavior of networks. However, the use of microgels as models for macroscopic networks within these experiments is strongly restricted. For instance, simple elongation experiments for the determination of the dynamic moduli must fail due to the molecular nature of microgels. Contrary to that, dynamic shear experiments can yield spectra that coincide with those of macroscopic networks, if the mechanical perturbations are restricted to short times (compared to the rotational relaxation time of the complete sphere) and small strains.

In addition, the measurements have to be performed for different microgel sizes at constant cross-linking density in order to investigate the influence of surface effects. Within the applied frequency window no size dependence of the spectra could be detected.

Figure 6 presents the storage modulus, G', the loss modulus, G'', and the dynamic viscosity, η^*, of sample A10/1 at a reference temperature of 150 °C. Starting from high frequencies where the glass transition influences the spectra, we observe the typical elastic plateau in G' of a rubbery material. The slope of η^* is close to −1, which is

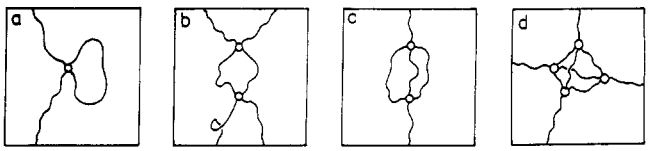

Figure 7. Four exemplary network defects, which should occur during cross-linking: (a) loop; (b) double bond; (c) triple bond; (d) separated cross-linked subunit.

the limiting value for a material with an "infinite" zero-shear viscosity. This is the experimental verification for the obvious assumption that spherical microgels of this size exhibit a very low overall mobility in the melt. The situation changes for higher strains (larger than 20%): the dynamic viscosity strongly drops, thus indicating the sliding of the molecules along their surfaces. At longer times corresponding to small frequencies, G'' also reaches a limiting value. This special microgel with the highest cross-linking density exhibits a very small limit of G'', which amounts to 3% of $G_N°$ only, the plateau value of G'. The response of this system is nearly completely elastic; 97% of the stored energy is recovered.

This spectrum also contains important structural information: from the plateau value we can calculate a mechanically effective cross-linking density, according to eq 6:

$$G_N° = A\frac{\rho RT}{M_c'} \tag{8}$$

A is the numerical factor on the order of unity, which depends on the theoretical treatment; since these data are best described with the Graessley theory, we adopt $A = 0.5$. This value is also in agreement with results obtained from PDMS model networks where a value of $A \approx 0.6$ is determined from stress–strain experiments.[31] The application of eq 8 is restricted by the theoretical assumption that the distribution of chain segments between the cross-links is described by a Gaussian function; i.e., the chains are totally flexible. This assumption certainly does not hold for the highly cross-linked microgel samples; due to effects of chain stiffness, these microgels are expected to exhibit higher moduli than predicted by eq 8. Nevertheless, the calculated cross-linking density is smaller than the chemical cross-linking density or, in other words, the mechanically effective M_c' is twice the M_c determined by the chemical composition. This comparison does not consider the presence of entanglements, the effect of which leads to an even smaller mechanical efficiency.

The origin of this inefficiency is also not known, but it is probably caused by the same phenomena that lead to the large-scale fluctuations of the cross-linking density as observed in the light-scattering experiments at low cross-linking densities. However, it must be recapitulated that this inefficiency is hardly seen in the absolute value of the swelling ratio, which is on the order of the expected value; it is just observed in quantities that are related to the heterogeneity of the structure only. We have speculatively attributed this behavior to a topological network structure that is not a grid-type one. Such structures could also explain the reduced plateau moduli since a reduced number of chains are involved in the strain.

All arrangements in which the cross-linking centers are not connected to four *different* neighboring centers exhibit a reduced "cycle rank"[43] and therefore lose elastic efficiency as well. Figure 7 illustrates simple substructures that are possibly present in those cross-linked structures. The latter three could explain the experimental observations: they are nearly invisible in swelling experiments since the polymer density remains unchanged, and they produce

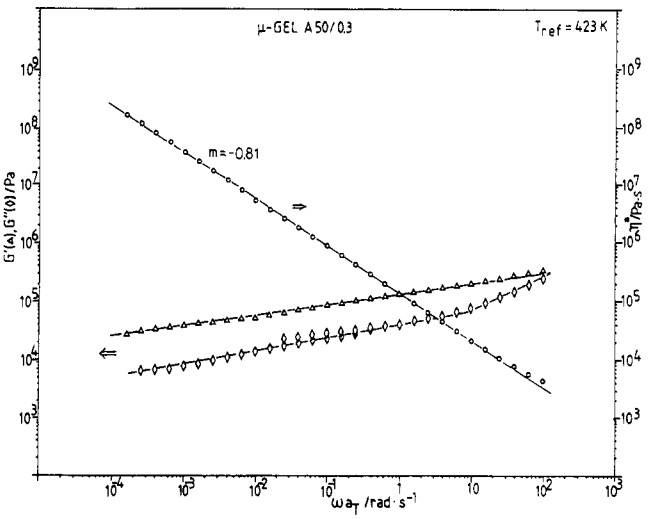

Figure 8. Master curve for sample A50/0.3 of the storage modulus, G' (△), the loss modulus, G'' (◇), and the dynamic viscosity, η^* (○), shifted to a reference temperature of T_{ref} = 423 K.

fluctuations on a larger scale than the elementary chain units. In addition, for entropic reasons a grid-type arrangement does not appear very probable; moreover, it is straightforward to assume a number of topological "defects" in the sense of Figure 7. The here presented cross-linking reaction via copolymerization seems to tend toward some "cooperativity" of the formed cross-links.

A further discussion on the basis of this restricted data set remains speculative, unless more experimental evidence is known. An extension of numerical calculations[41] to defect other than loops would surely throw more light on their local appearance in dependence of the cross-linking conditions. From an experimental point of view, the connectivity of the structure will be further investigated in a forthcoming paper by experiments close to the gel transition where different defects may become distinguishable.

Finally, Figure 8 presents the dynamic mechanical spectrum of sample A50/0.3, which has been prepared in the presence of 70% solvent. Instead of an elastic plateau, we obtain a constant decrease of the moduli toward lower frequencies. Since we observe the motion of small-chain segments at high frequencies and the response of larger substructures at longer times, the evolution of the elastic force is traced on different size scales. In this figure no pronounced relaxation time is observable that can be accorded to a loss mechanism. Moreover, the moduli become smaller over the whole frequency range. This could be interpreted by "defects" with a continuous size, i.e., cyclic substructures with various cycle ranks.

The frequency dependences of G' and G'' in this double-logarithmic plot are described by straight lines over more than 5 decades of frequency and is only limited at the low-frequency side by the resolution of the rheometer. Such a behavior is also known from microgels synthesized below the gel point[44] and, with a different slope, from macroscopic networks at the gel point. In the latter case, it is theoretically explained by a fractal structure of the system.

Therefore, we conclude from Figure 8 that cycles on all different size scales are formed due to dilution: we do not recognize distinct loss peaks but observe a continuous loss over the whole frequency range. The probability of formation of different cycle sizes corresponds to distinct laws of formation: the envelope of all loss mechanisms produces a straight line. In other words, the system shows a behavior of a critical structure at or close to the gel point;

the formation process of cyclic substructures must be self-similar in the vicinity of this "phase transition" of gelation. This is experimentally proven by the shape of the spectrum of sample A50/0.3. Like the data of the swelling ratios also the dynamic mechanical measurements unambiguously show that the influence of dilution on the cross-linking reaction is inadequately described by introduction of a simple geometric memory term h. More detailed information about microgel systems close to the gel transition will be more extensively presented in our next paper concerning the behavior of micronetworks.

(IV) Conclusion

Microgels synthesized by radical copolymerization in microemulsion can be treated as small, spherical network particles with molecular weights between $50 \times 10^6 < M_w < 1 \times 10^9$. They are easy to handle and are readily characterized by the methods of polymer analysis in solution, e.g., viscosimetry or static and dynamic light scattering.

From the intrinsic viscosity data, a "molecular" swelling ratio can be calculated that depends on the cross-linking density of the microgels in the same manner as known from macroscopic networks. These data are best described by the theoretical work of Duiser–Staverman or Graessley; these treatments are also used to calculate an apparent efficiency of cross-linking.

The light-scattering results agree very well with the solution viscosity experiments. However, from the combination of static and dynamic light scattering we can determine a heterogeneity of swelling even on the intermediate size scale offered by the microgel dimensions. The dimensional scale of this heterogeneity is large compared to the primary chain or to a mesh of the network. A possible explanation for such a behavior can be found in nonideal topological arrangements of cross-linking centers, especially for cross-linking via copolymerization, which is known to exhibit quite a peculiar behavior.

Application of microgels as models for cross-linked structures has been extended to two further investigations. On the one hand, we have demonstrated that a lower efficiency of cross-linking has to be assorted with flexible cross-linking agents, which is possibly due to the formation of very small rings. On the other hand, we have examined the influence of dilution during the cross-linking reaction. Also in this case, the apparent efficiency is successively lowered when more diluent is added. We have assigned this behavior to the formation of cross-links incorporated in structures with a reduced cycle rank.

Dynamic mechanical shear experiments on microgels in the melt result in spectra of the storage and the loss modulus, which are comparable to those of macroscopic networks, when small strains and perturbations are short compared to the overall rotation applied. Also in these experiments, indications for nonideal cross-linking arrangements are present; in the case of a sample with a very high cross-linking density (10 monomer units between cross-links), the experimental plateau value reaches just 45% of the theoretically expected one. Dilution during the cross-linking reaction alters the mechanical master curves in a characteristic way. Instead of a plateau, a constant decrease of the moduli with decreasing frequency is obtained. A similar, but more pronounced, behavior is known from network systems close to the gel transition.

Beyond all doubt, more experimental evidence is needed for a decisive answer about the cross-linking topology. In an extension of this work, we plan to perform small-angle neutron scattering on these microgels; also the examinations have to be extended to a variation of the microgel size. Nevertheless, the aim of this first paper was to demonstrate that microgels may present an additional experimental access for analyzing the behavior and the physics of all cross-linked systems.

Acknowledgment. We especially thank H. Sillescu for many helpful comments and discussions. We are also indebted to T. Pakula for his competent help in context with mechanical experiments and B. Schupp and C. Rosenauer for technical help during the synthetic part of the work. Financial support by the Deutsche Forschungsgemeinschaft, the Max-Planck Gesellschaft, and the Böhringer-Ingelheim Stiftung is gratefully acknowledged.

References and Notes

(1) Boue, F.; Bastide, J.; Buzier, M.; Collette, C.; Lapp, A.; Herz, J. *Prog. Colloid Polym. Sci.* **1987**, *75*, 152.
(2) Ferry, J. D. *Viscoelastic Properties of Polymers*, 3rd ed.; Wiley: New York, 1980.
(3) Nimtz, G.; Marquardt, P.; Stauffer, D.; Weiss, W. *Science* **1988**, *242*, 1671.
(4) Staudinger, H.; Husemann, E. *Ber.* **1935**, *68*, 1618.
(5) Hoffmann, M. *Makromol. Chem.* **1974**, *175*, 613.
(6) Hild, G.; Okasha, R. *Makromol. Chem.* **1985**, *186*, 389.
(7) Atik, S. S.; Thomas, J. K. *J. Am. Chem. Soc.* **1982**, *104*, 5868.
(8) Johnson, P. L.; Gulari, E. *J. Polym. Sci., Polym. Chem. Ed* **1984**, *22*, 3967.
(9) Candau, F. *Encycl. Polym. Sci. Eng.* **1986**, *9*, 718.
(10) Ferrick, M. R.; Murtagh, J.; Thomas, J. K. *Macromolecules* **1989**, *22*, 1515.
(11) Schulman, J. E.; Stoeckenius, W.; Prince, L. *J. Phys. Chem.* **1959**, *63*, 1677.
(12) Clausse, M.; Peyrelasse, J.; Boned, C.; Heil, J.; Nicolas-Morgantini, L.; Zradba, A. In *Surfactants in Solution*; Mittal, K. L., Lindman, B., Eds.; Plenum Press: New York, 1984; Vol. III, p 1583.
(13) Antonietti, M.; Bremser, W.; Schmidt, M., to be published.
(14) Michel, J., private communication.
(15) Bantle, S.; Schmidt, M.; Burchard, W. *Macromolecules* **1982**, *15*, 1604.
(16) Antonietti, M.; Sillescu, H.; Schmidt, M.; Schuch, H. *Macromolecules* **1988**, *21*, 736.
(17) Bremser, W. Diplomarbeit, Mainz, 1988.
(18) Takahashi, A.; Kawaguchi, M. *Adv. Polym. Sci.* **1982**, *46*, 1.
(19) Yamakawa, H. *Modern Theory of Polymer Solutions*; Harper & Row: New York, 1971.
(20) Scheraga, H. A.; Mandelkern, L. *J. Am. Chem. Soc.* **1953**, *75*, 179.
(21) Burchard, W.; Schmidt, M. *Macromolecules* **1981**, *14*, 210.
(22) Oseen, C. H. *Neuere Methoden und Ergebnisse in der Hydrodynamik*; Akademie Verlag: Leibzig, 1927.
(23) Schmidt, M.; Nerger, D.; Burchard, W. *Polymer* **1979**, *20*, 582.
(24) Rempp, P.; Herz, J.; Borchard, W. *Adv. Polym. Sci.* **1978**, *26*, 107.
(25) Flory, P. J.; Wall, F. T. *J. Chem. Phys.* **1951**, *19*, 1435.
(26) Hermans, J. J. *Trans. Faraday Soc.* **1947**, *43*, 591.
(27) James, H. M.; Guth, E. *J. Chem. Phys.* **1943**, *11*, 455; **1953**, *21*, 1039.
(28) Graessley, W. W. *Macromolecules* **1975**, *8*, 189; **1976**, *9*, 865.
(29) Duiser, J. A.; Staverman, J. A. *Physics of non-crystalline Solids*; North Holland, Amsterdam, 1965.
(30) Noda, I.; Higo, Y.; Ueno, N.; Fujimoto, T. *Macromolecules* **1984**, *17*, 1055.
(31) Mark, J. E. *Adv. Polym. Sci.* **1982**, *44*, 1.
(32) Mark, J. E.; Llorente, M. A. *J. Am. Chem. Soc.* **1980**, *102*, 632.
(33) Flory, P. J. *J. Am. Chem. Soc.* **1941**, 63, 3083, 3091, 3096. Stockmayer, W. H.; *J. Chem. Phys.* **1943**, *11*, 45.
(34) Straehle, W.; Seitz, U.; Funke, W. *Angew. Makromol. Chem.* **1977**, *60*, 111.
(35) Antonietti, M.; Ehlich, D.; Fölsch, K. J.; Sillescu, H.; Schmidt, M.; Lindner, P. *Macromolecules* **1989**, *22*, 2802.
(36) Flory, P. J. *Principles of Polymer Chemistry*; Cornell University Press: Ithaca, NY, 1953.
(37) Johnson, R. M.; Mark, J. E. *Macromolecules* **1972**, *5*, 41.
(38) Soper, B.; Harvard, R. N.; White, E. F. T. *J. Polym. Sci., Part A1* **1972**, *10*, 2545.
(39) Schmidt, M.; Burchard, W. *Macromolecules* **1981**, *14*, 370.
(40) Ilavsky, M.; Dusek, K. *Macromolecules* **1986**, *19*, 2139.

(41) Lee, K. J.; Eichinger, B. E. *Macromolecules* **1989,** *22,* 1441.
(42) Dusek, K. In *Developments in Polymerization*; Harward, R. N., Ed.; Applied Science: Barking, U.K., 1982; Vol. 3.
(43) Flory, P. J. *Macromolecules* **1982,** *15,* 99.
(44) Antonietti, M.; Fölsch, K. J.; Sillescu, H.; Pakula, T. *Macromolecules* **1989,** *22,* 2812.

Registry No. (Styrene)(*m*-DIB) (copolymer), 26124-82-3.

Effect of Surrounding Medium on Intramolecular Conformational Changes in Probe Molecules

Ivet Bahar* and Burak Erman

Polymer Research Center and School of Engineering, Bogazici University, Bebek 80815, Istanbul, Turkey

Lucien Monnerie

Laboratoire de Physicochimie Structurale et Macromoléculaire, associé au CNRS, ESPCI, 10 rue Vauquelin, 75231 Paris, France

Received November 13, 1989; Revised Manuscript Received February 12, 1990

ABSTRACT: Conformational dynamics of short probes dispersed in a matrix is investigated. The matrix can be in two states, fast or slow, depending on the amount of free volume. Following the work of Anderson and Ullman,[4] the amount of free volume is assumed to fluctuate in time, thus modifying the states of the matrix. The probe undergoes transitions between two states resembling trans–cis isomeric transitions. Correlation times of the probe–matrix system exhibit a clear transition as the free-volume fluctuations of the matrix become faster. In a fast matrix, the temperature dependence of correlation times for probes reflects both the intramolecular conformational barrier in the probe and the energy change of viscous origin in the matrix, while in a slow matrix only the activation energy of the matrix is observed. This is in agreement with the results from recent experiments with fluorescent probes dissolved in small-molecule solvents and in bulk polymer.

Introduction

Intramolecular excimer formation in fluorescent probe molecules has been shown to give information about the dynamics of the environment in which they are dispersed in small quantities.[1] A large body of experimental work confirms the efficiency of this technique in understanding the dynamics of various size molecules, ranging from small solvent molecules to polymers in the bulk state.

In general, the internal reorientation of the probe is opposed both by intramolecular conformational barriers and by intermolecular resistance of viscous origin. In fact, in a matrix of small or oligomeric molecules, the activation energy for the motion of the probe is observed from experiments to be equal to the sum of (i) the activation energy for intramolecular rotameric transitions of the probe and (ii) the one associated with the viscosity of the environment.[2] For probes dispersed in a bulk polymer, however, the temperature dependence of the probe motion is characteristic of the surrounding medium only; i.e., the mobility of the bulk polymer is the factor almost totally controlling the motion of the probe. The specific aim of the present paper is to investigate, theoretically, the cause of this change in the observed activation energies or in the extent of probe–matrix coupling depending on the mobility of the surroundings.

A first description of a coupling of this nature is given by the defect diffusion model of Glarum.[3] The model describes the cooperativity between an orienting molecule and its environment. The orientation of the molecule is more likely immediately after one of its neighbors relaxes. The relaxing neighbor is treated as a defect that may diffuse toward the reorienting molecule. The diffusion coefficient associated with the motion of the defect describes the mobility of the environment. The defect diffusion model was further explored, in a more refined way, by Anderson and Ullman.[4] According to this model, the environment about each molecule is taken to fluctuate with time. These fluctuations are assumed to critically affect the reorientation probabilities of the molecule. The fluctuations of the environment are associated with fluctuations of free volume. The work of Anderson and Ullman is the first rigorous attempt in establishing the dynamic nature of the free-volume effect in intermolecular correlations. The concept of a fluctuating environment was further treated by Anderson[5] in terms of a "simple defect" model. According to this model, the environment of a given molecule can be in either of two states. One of the states is "unyielding". A molecule in this state has a small probability of reorientation. The second state constitutes a defect in which the molecule has a high probability of reorienting. The motion of the molecule may in its most general form be described in terms of the well-known Ornstein–Uhlenbeck process as shown by Anderson and Ullman. A similar treatment has been employed by Sillescu[6] as well, in describing magnetic spin resonance line shapes in liquids with molecular reorientation. In the present study, we reconsider the dynamics of a probe molecule by solving the master equation for a rotational jump model in which the rates of internal transitions of the probe molecule depend on the state of its immediate surrounding. The formulation though less formal than that of Anderson–Ullman and Sillescu helps for a clear

0024-9297/90/2223-3805$02.50/0